
The Key Role of Headrest Optimization in Driver Comfort

Hamid Gheibollahi and Masoud Masih-Tehrani

Vehicle Dynamical System Research Lab, School of Automotive Engineering, Iran University of Science and Technology, Tehran, Iran.

Mohammadmehdi Niroobakhsh

Civil & Mechanical Engineering Department, University of Missouri-Kansas City, Kansas City, USA.

(Received 9 August 2017; accepted 5 September 2018)

In this study, adding a headrest to the conventional vehicle driver seat is investigated to improve the driver comfort and decrease the driver damages. For this purpose, a conventional biomechanical human body model of whole-body vibrations is provided and modified by adding a head degree of freedom to the body model and a headrest to the seat model. The basic model is in the sitting posture, lumped parameters and has nine DOFs for the human body, on contrary to the proposed model which has ten DOFs. The new human body DOF is the twisting motion of the head and neck. This new DOF is generated because of headrest adding to the driver's seat. To determine the head discomforts, the Seat to Head (STH) indexes are studied in two directions: horizontal and vertical. The Genetic Algorithm (GA) is used to optimize the STH in different directions. The optimization variables are stiffness and damping parameters of the driver's seat which are 12 for the basic model and are 16 for a new seat. The integer programming is used for time reduction. The results show that new seat (equipped by headrest) has very better STH in both directions.

NOMENCLATURE

| | |
|----------------------|--|
| c_{1v}, c_{1h} | Upper leg vertical and horizontal dampers, |
| c_{2v}, c_{2h} | Pelvic vertical and horizontal dampers, |
| c_{4v}, c_{4h} | Back horizontal and vertical dampers, |
| $c_{21} \sim c_{54}$ | The respective dampers between body segments, |
| C | Damping matrix, |
| f | Force vector, |
| F | Complex Fourier transform of the forces, |
| k_{1v}, k_{1h} | Upper leg vertical and horizontal springs, |
| k_{2v}, k_{2h} | Pelvic vertical and horizontal springs, |
| k_{4v}, k_{4h} | Back horizontal and vertical springs, |
| $k_{21} \sim k_{54}$ | The respective springs between body segments, |
| K | Stiffness matrix, |
| l | Distance from headrest to the neck joint, |
| m_1 | Mass of Upper Leg (left + right), |
| m_2 | Mass of Pelvic, |
| m_3 | Mass of Viscera (Soft abdominal body parts), |
| m_4 | Mass of upper Torso (Including hands), |
| m_5 | Mass of head and neck, |
| M | Mass matrix, |
| STH | Head to seat vibration ratio (vertical), |
| STH_x | Head to seat vibration ratio (Horizontal), |
| STH_{RMS} | Root mean square of STH , |
| w_1 | Transferability weighting coefficients of horizontal vibrations, |
| w_2 | Transferability weighting coefficients of horizontal vibrations, |
| x | Complex transfer response vector, |
| X | Complex Fourier transform of the variables, |
| X_0 | Seat input excitation in the vertical direction, |
| X_8 | Back horizontal frequency response, |
| X_9 | Head vertical frequency response, |

X_b Backrest horizontal excitation,

Θ Head twist angle,

ω Excitation frequency.

1. INTRODUCTION

The experience of whole-body vibration in daily life is common to most people. It happens when a person is affected by a vibrating surface and thus, all parts of the body that may even be far from the main vibration source are exposed to the vibration. Whole-body vibration at frequencies from 1 to 100 Hz for humans is understandable. Backbone damage caused by long-term vibrations occurs in the frequency range of 4 to 12 Hz. Feeling terrible in the digestive system is a result of being exposed to whole-body vibrations for long periods of time. This inconvenient feeling in the stomach occurs at frequencies between 4 to 5 Hz. This is the resonance range of the stomach. The cardiovascular system can be affected by long-term of whole-body vibrations at frequencies below 20 Hz. Fast and deep breathing, in addition to increased heart rate, are the results of these vibrations.¹ The resonance frequency for the head and neck is variable from 4 to 13 Hz.² Many studies are performed to improve driver comfort with headrest optimization.³⁻⁵

Biomechanical studies of body vibration and its damage are conducted on humans, animals, and dummies. These studies on humans date back to 1918, when Hamilton investigated the effect of vibrations on limestone mine workers.⁶ The reason for choosing dummies is to prevent human injuries.⁷ In 1984, Alem determined a standard for these damages by performing the axial impact test on nineteen human corpses to study the mechanical properties of the head, neck and spine.⁸ In 1998,

in an effort by Boileau overall biodynamical human body response values facing different workplaces were specified from various published data.⁹ In 2000, Yoganandan studied the biomechanical body responses of a man and four women in crashes applied to the rear of the body and evaluated neck injury risks.¹⁰ In 2005, Mansfield pointed out in his book that, for whole-body vibrations, people are more sensitive to frequencies below 20 Hz.¹¹ In 2008, Nelisse and Patra designed two dummies to assess the vibration isolation effectiveness of suspension seats.¹² In 2010, Bovenzi conducted some tests on 202 male drivers. His goal was to address injuries and back pains caused by long distance driving.¹³ In 2013, Thamsuwan and his colleagues studied whole-body vibrations of bus drivers with different floor heights of buses and considered their back pain at each height.¹⁴ In 2014, Zhao and his colleagues designed a semi-active control system to control vibrations on the human body by using a four DOFs of the human body model.¹⁵

Another method in these studies involves the use of biomechanical human body models.^{16–18} These models can be classified into lumped-parameter models, multi body models and finite element models.^{19–22} In lumped-parameter models, the human body is considered as several concentrated masses that are connected with springs and dampers. Multi body models are composed of several rigid bodies that are connected to each other by either pin connection (two-dimensional) or spherical connection (three-dimensional). For finite element models, it is assumed that the human body contains many finite elements and that the properties of these elements are obtained from experiments on human bodies.

One application of biomedical studies is designing an optimized driver's seat to reduce body vibrations.²³ Models with this purpose usually consider the optimal parameters for a driver's seat. However, the headrest and horizontal vibrations applied to the head in long distance traveling is very important.²⁴ Vibrations caused by the driver's headrest during long distance travel can cause damage to the upper vertebrae of the spine, head and neck.

In this study, Harsha and his colleague's model which was introduced in 2014, was chosen as the base model for the human body and driver's seat.²⁵ The reason for this selection was that this model contained both vertical and horizontal degrees of freedom simultaneously and a lumped-parameter that is rarely found in other models. Harsha's model has nine DOFs and vibrations applied to the body in horizontal and vertical directions. However, in his model the effect of input vibrations from the base to the head were not considered and input vibrations were from the seat and backrest of the driver. Also, in Harsha's model the horizontal DOF of the head was dependent on waist movement and has no independent DOF.²⁵

To add the headrest and study passenger comfort, vibrations applied to head were modeled in horizontal and vertical directions and the body had ten DOFs. Then, a biomechanical model of the body and seat was introduced and the governing equations of the base and modified model were derived. The optimization problem to evaluate the passenger's comfort was extracted and its solution was expressed by a genetic algorithm method. Due to the complexity of the problem and the large number of DOFs (12 optimization variable for the base model

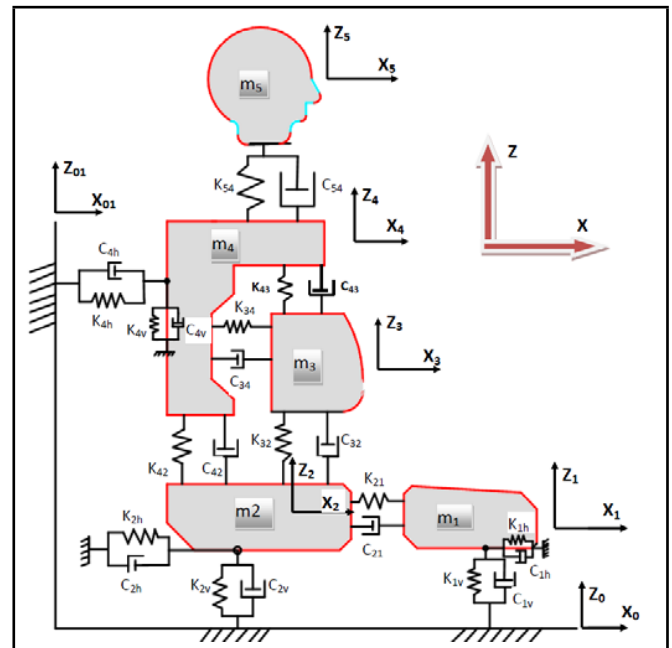


Figure 1. Nine DOFs Harsha's biomechanical model of the human body.²⁵

and 16 variables for the new model) using this powerful algorithm was an appropriate option. Finally, the optimization results were reviewed and classified.

2. MODELING AND METHODOLOGY

In this study, a biomechanical model of whole-body vibration was provided. This model was provided to check head injuries caused by vibrations and finally to design the optimal parameters for the car's seat. The presented model was in a sitting position, lumped parameter and had ten DOFs. Applied vibrations on model were both vertical and horizontal. The overall structure of the model was obtained from the nine DOFs of Harsha's model.²⁵ In Harsha's model, the body was divided into five concentrated mass that each had two DOFs in horizontal and vertical directions. However, it should be noted that, in Harsha's model, the horizontal DOF of the head is associated with the horizontal movement of the waist and cannot be considered as an independent DOF. Furthermore, in Harsha's model the forces that were applied on the body came from the seat and the backrest. Figure 1 shows Harsha's model with the backrest. In addition to the above forces, the horizontal force applied to the head was also considered. In this way, one rotational DOF was added to the vertical movement of the head that increased DOFs from nine to ten. Figure 2 shows the proposed model in this study. In this paper, the motion equations of the model were extracted and then, by transferring them from time to frequency domain, the vibration transferability parameter from seat to head in the presence of headrest was discussed. Afterward, by defining an objective function of vibration transferability and using a genetic algorithm, seat parameters were optimized.

2.1. Governing Equations of Modeling

In general, there are two methods for solving motion equations: solving in time domain and solving in frequency domain. Usually solving in frequency domain is more efficient

Table 4. Optimization variables for the proposed model (with headrest).

| Parameter | Value |
|---------------------|--|
| Number of variables | 16 |
| Variables | $[k_{1v}, k_{1h}, k_{2v}, k_{2h}, k_{4v}, k_{4h}, k_{5v}, k_{5h}, c_{1v}, c_{1h}, c_{2v}, c_{2h}, c_{4v}, c_{4h}, c_{5v}, c_{5h}]$ |
| Lower bound | [1600(N/m) 1(N/m) 15162(N/m) 90(N/m) 1720(N/m) 230(N/m) 1500(N/m) 400(N/m) 10(Ns/m) 1(Ns/m) 4(Ns/m) 1(Ns/m) 33(Ns/m) 15(Ns/m) 30(Ns/m) 50(Ns/m)] |
| Upper bound | [160000(N/m) 150(N/m) 1516200(N/m) 9000(N/m) 172000(N/m) 23000(N/m) 150000(N/m) 40000(N/m) 1050(Ns/m) 140(Ns/m) 470(Ns/m) 150(Ns/m) 3300(Ns/m) 1500(Ns/m) 3000(Ns/m) 5000(Ns/m)] |

Table 5. Optimization properties for the base model (without headrest).

| Parameter | Value |
|---------------------|---|
| Number of variables | 12 |
| Variables | $[k_{1v}, k_{1h}, k_{2v}, k_{2h}, k_{4v}, k_{4h}, c_{1v}, c_{1h}, c_{2v}, c_{2h}, c_{4v}, c_{4h}]$ |
| Lower bound | [1600(N/m) 1(N/m) 15162(N/m) 90(N/m) 1720(N/m) 230(N/m) 10(Ns/m) 1(Ns/m) 4(Ns/m) 1(Ns/m) 33(Ns/m) 15(Ns/m)] |
| Upper bound | [160000(N/m) 150(N/m) 1516200(N/m) 9000(N/m) 172000(N/m) 23000(N/m) 1050(Ns/m) 140(Ns/m) 470(Ns/m) 150(Ns/m) 3300(Ns/m) 1500(Ns/m)] |

is proved analytically and empirically that genetic algorithms are a potent tool in uncertain environments. Initial populations in which genetic operators are applied are defined as a chromosome string. Populations from generation to generation are recovered by applying genetic operators such as crossover and mutation and are led to the optimal population. The crossover operation involves taking two chromosomes as parents. Their combination produces two children to search the entire space by the algorithm. However, the goal of mutation operation is to create diversity in populations. An objective function plays a selector role in the populations. The optimization variables properties are listed in Tab. 4 for the proposed model (with headrest) and in Tab. 5 for the base model (without headrest).

In this study, MATLAB software was used for genetic algorithm purpose. In the MATLAB software, the input variables were the seat’s stiffness and damping matrices. The number of them for Harsha’s model was 12 and for the provided model were 16. Also, equality and inequality constraints were ignored. It should be noted that the lower and upper bounds for the stiffness and damping’s input variables were considered 10% and ten times the default values of stiffness and damping. Furthermore, the nonlinear conditions were neglected. For faster calculations, variables chosen by the software were intended integers.^{31,32} The Genetic algorithm parameters were introduced in Tab. 6. These parameters were the same for both models’ optimization.

Two objective functions were used to run the software. Equations (7) and (8) show the objective functions of the optimization. In Eq. (7), the amount of root means square for vertical and horizontal vibrations with their weighting coefficients were provided. Equation (8) shows the maximum horizontal and vertical vibration portability with their weighting

Table 6. Genetic algorithm parameters.

| Parameter | Description | Value |
|-----------------------|--|----------------------------------|
| Population Type | Data type of the population. | “Bit string” and “Double vector” |
| Population Size | Size of the population. | 50 |
| Elite Count | Positive integer specifying how many individuals in the current generation are guaranteed to survive to the next generation. | 3 |
| Crossover Fraction | The fraction of the population at the next generation, not including elite children that is created by the crossover function. | 0.8 |
| Migration Fraction | Scalar between 0 and 1 specifying the fraction of individuals in each subpopulation that migrates to a different subpopulation. | 0.2 |
| Max Generations | The maximum number of iterations before the algorithm halts. | 300 |
| Time Limit | The algorithm stops running after Time Limit seconds. | Inf |
| Max Stall Generations | The algorithm stops if the average relative change in the best fitness function value over Max Stall Generations is less than or equal to Function Tolerance. If Stall Test is “Geometric Weighted”, then the algorithm stops if the weighted average relative change is less than or equal to Function Tolerance. | 50 |
| Tol Fun | The algorithm stops if the average relative change in the best fitness function value over Max Stall Generations is less than or equal to Tol Fun. | 1×10^{-6} |
| Tol Con | Determines the feasibility concerning nonlinear constraints. | 1×10^{-3} |

coefficients.

$$y = w_1 \text{RMS}(STH_x) + w_2 \text{RMS}(STH); \quad (7)$$

$$y = w_1 \max(STH_x) + w_2 \max(STH); \quad (8)$$

where w_1 and w_2 were transferability weighting coefficients of vertical and horizontal vibrations so that their sum was equal to one and each of them was smaller than one. Given that the human body has the highest vibration sensitivity in the frequency range of 4-8 Hz in vertical vibrations and the frequency range of 1-2 Hz in horizontal vibrations,³³ in calculating all of these functions, the filtered value of these vibrations was measured in the listed intervals.

3. CHARTS AND RESULTS

According to the mentioned objective functions, vibration optimization was performed for Harsha’s model and the proposed model. In the above equations, w_1 and w_2 were considered equal to 0.5. If the objective function is Eq. (7), Fig. 3 compares the transferability of horizontal and vertical vibrations in Harsha’s model and the optimized one.

As it is shown in Fig. 3, the maximum transferability of horizontal and vertical vibrations in Harsha’s optimized model is reduced significantly compared to the Harsha’s model. In Fig. 4, vibration transferability is optimized in the proposed model, and also reduction of maximum vibration is quite evident in that. In Fig. 5, the optimal amount of horizontal and vertical vibrations in Harsha’s model and the proposed model is compared. Based on the results of the graph, it is found that

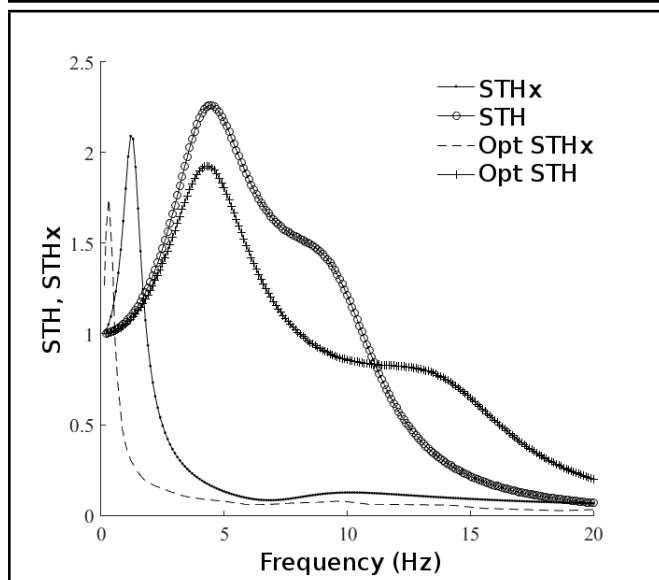


Figure 3. Optimization of horizontal and vertical vibrations transmission in Harsha's model with Eq. (7).

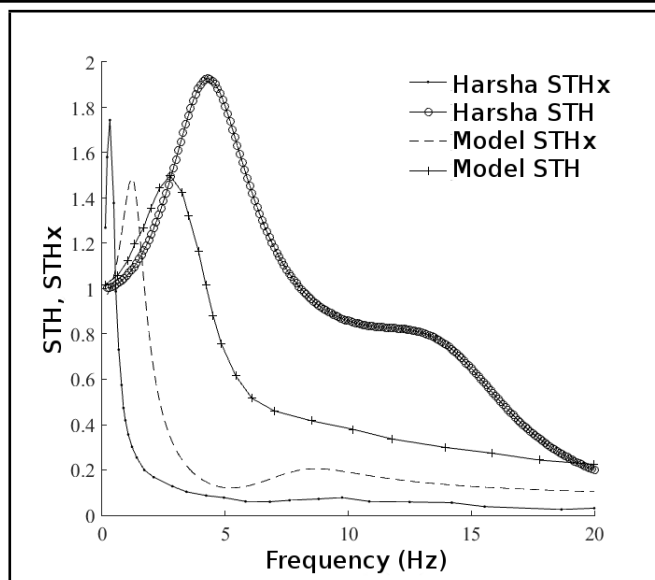


Figure 5. Compare optimization of horizontal and vertical vibrations transmission in the presented model by Harsha's model with Eq. (7).

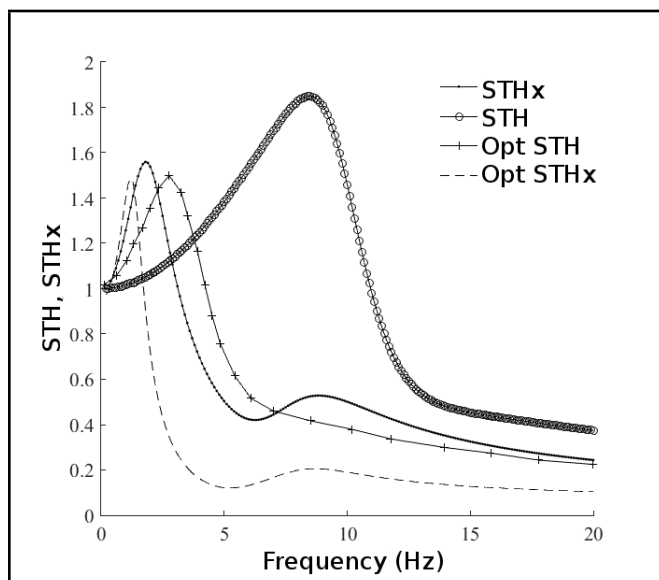


Figure 4. Optimization of horizontal and vertical vibrations transmission in the presented model with Eq. (7).

the root means square values for horizontal and vertical vibrations transferability the optimized Harsha's model are respectively equal to 0.64 and 1.05. The values for this parameter in the optimized proposed model, which are reduced, are respectively equal to 0.4 and 0.95. Also, the maximum transferability of horizontal and vertical vibrations in the optimized Harsha's model is respectively equal to 1.73 and 1.93, while the value of this parameter in the optimized proposed model is respectively equal to 1.48 and 1.49.

In Tabs. 7 and 8, the value of first and optimized stiffness and damping parameters are given for both Harsha's model and the proposed model. It should be noted that these values are calculated for the objective function of Eq. (7).

In the following, the optimal values for both Harsha's model and proposed model are given, if the objective function is Equation (8). Figure 6 shows horizontal and vertical vibrations' transferability despite this objective function.

Table 7. The primary and optimal of seat stiffness and damping parameters for Harsha's model in Eq. (7).

| Parameter | Unit | Harsha's model | Optimal |
|-----------|------|----------------|---------|
| k_{1v} | N/m | 1600 | 116486 |
| k_{1h} | N/m | 15 | 15 |
| k_{2v} | N/m | 151625 | 1159330 |
| k_{2h} | N/m | 905 | 4184 |
| k_{4v} | N/m | 17200 | 54390 |
| k_{4h} | N/m | 2300 | 10543 |
| c_{1v} | Ns/m | 104.35 | 396 |
| c_{1h} | Ns/m | 14 | 36 |
| c_{2v} | Ns/m | 47 | 323 |
| c_{2h} | Ns/m | 15 | 123 |
| c_{4v} | Ns/m | 324.5 | 2751 |
| c_{4h} | Ns/m | 154 | 1317 |

As seen in Fig 6, the maximum value of the vertical and horizontal vibration transferability in the optimized Harsha model has been reduced compared to the original Harsha model. In Fig 7, the vibration transferability in the proposed model and its optimized model is observed. It is evident that the value of the maximum vibration transferability parameter in both horizontal and vertical directions is reduced. In Fig. 8, the optimum value of horizontal and vertical vibrations is compared with both Harsha's model and the proposed model concerning the new objective function. According to the results of Fig. 8, it is found that the root means square for vertical and horizontal vibrations transferability in Harsha's optimized model are respectively 0.89 and 0.78. The values of these parameters, which have been reduced, for the optimized proposed model are respectively 0.93 and 0.37. Also, the maximum vertical and horizontal vibrations transferability for Harsha's optimized model are respectively 1.79 and 1.20, while for the optimized proposed model have been calculated respectively 1.29 and 0.70.

In this section, both the basic and optimized values stiffness and damping parameters for the Harsha model and the proposed model were provided respectively. These values had been obtained for the objective function of Eq. (8). Tables 9 and 10 show the value of these parameters for the Harsha's

Table 8. The basic and optimal of seat stiffness and damping parameters for presented model in Eq. (7).

| Parameter | Unit | Presented model | Optimal |
|-----------|------|-----------------|---------|
| k_{1v} | N/m | 1600 | 91190 |
| k_{1h} | N/m | 15 | 103 |
| k_{2v} | N/m | 151625 | 686639 |
| k_{2h} | N/m | 905 | 5240 |
| k_{4v} | N/m | 17200 | 14991 |
| k_{4h} | N/m | 2300 | 230 |
| k_{5v} | N/m | 15000 | 2661 |
| k_{5h} | N/m | 4000 | 418 |
| c_{1v} | Ns/m | 104.35 | 766 |
| c_{1h} | Ns/m | 14 | 89 |
| c_{2v} | Ns/m | 47 | 279 |
| c_{2h} | Ns/m | 15 | 57 |
| c_{4v} | Ns/m | 334.5 | 2191 |
| c_{4h} | Ns/m | 154 | 16 |
| c_{5v} | Ns/m | 300 | 2726 |
| c_{5h} | Ns/m | 500 | 510 |

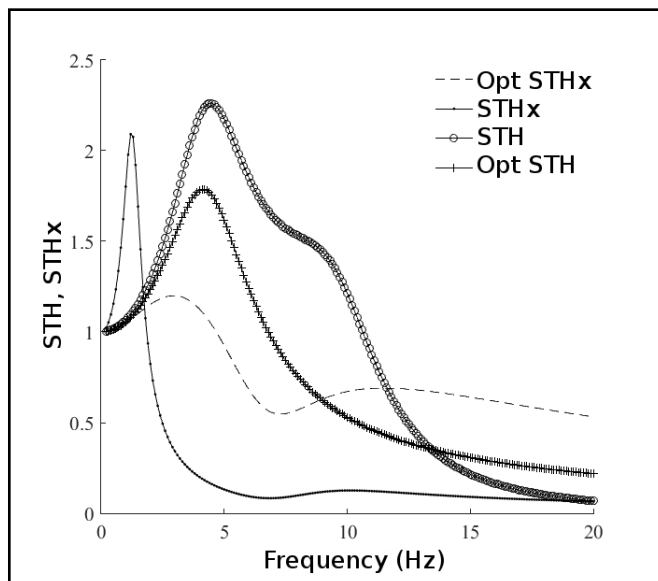


Figure 6. Optimization of horizontal and vertical vibrations transmission in Harsha's model with Eq. (8).

model and the proposed model respectively.

Table 11 shows the comparison of adding a headrest to different optimization scenarios. The first column shows the objective functions while two functions are mixed (vertical and horizontal directions) with two different weighting factor couples and other functions are clear (just vertical or just horizontal direction). The third column is the base model (without headrest), and the fourth column is the headrest equipped model. The results show the significant improvement in different objective functions, by adding the headrest.

4. CONCLUSION

In this article, the superiority of adding a headrest to the vehicle's seat has been investigated to improve the driver comfort. For this purpose, a biomedical model of whole-body vibration together with the seat's horizontal and vertical vibrations has been introduced to assess the damage caused by vibrations and optimize the vehicle's seat parameters. This model is in the sitting posture which is the lumped parameter model, and it had ten degrees of freedom. In the basic model, the head has independently no degree of freedom and swings

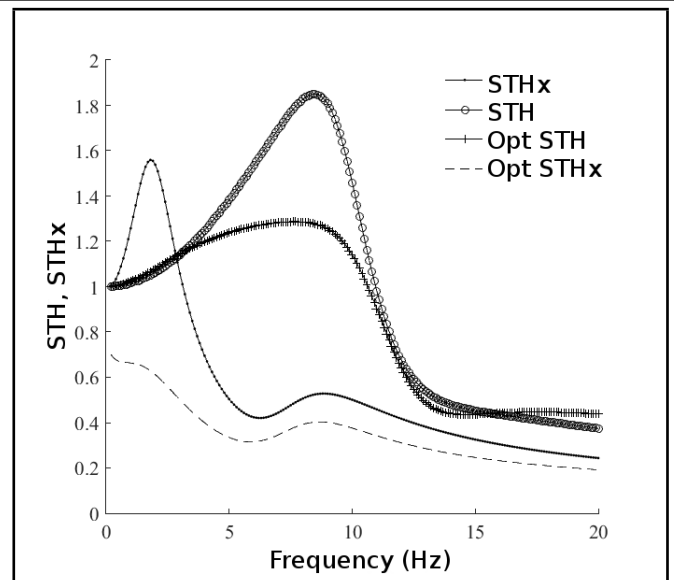


Figure 7. Optimization of horizontal and vertical vibrations transmission in the presented model with Eq. (8).

Table 9. The primary and optimal of seat stiffness and damping parameters for Harsha's model in Eq. (8).

| Parameter | Unit | Harsha's model | Optimal |
|-----------|------|----------------|---------|
| k_{1v} | N/m | 1600 | 11701 |
| k_{1h} | N/m | 15 | 30 |
| k_{2v} | N/m | 151625 | 15412 |
| k_{2h} | N/m | 905 | 8083 |
| k_{4v} | N/m | 17200 | 1733 |
| k_{4h} | N/m | 2300 | 22970 |
| c_{1v} | Ns/m | 104.35 | 14 |
| c_{1h} | Ns/m | 14 | 2 |
| c_{2v} | Ns/m | 47 | 465 |
| c_{2h} | Ns/m | 15 | 4 |
| c_{4v} | Ns/m | 324.5 | 2050 |
| c_{4h} | Ns/m | 154 | 1478 |

with the waist horizontally. In the new model, considering the backrest, the torsional movements of the head and neck are also considered. However, the base model has nine degrees of freedom and the headrest and horizontal force into the head are not modeled in it.

Also, with the definition of an objective function of transferability for head to seat vibrations and to use a genetic algorithm, seat parameters have been optimized. The presented results show that seat to head vibrations transferability in both horizontal and vertical direction has been improved by adding the headrest. According to the results in the previous section, these achievements can be concluded:

- The horizontal vibration transferability has been reduced up to 50% in comparison with the base model (without headrest), in different objective functions (RMS or maximum vibration transferability).
- The vertical vibration transferability has been reduced up to 50% in comparison with the base model (without headrest), in different objective functions (RMS or maximum vibration transferability).

In general, concerning the transferability reduction in both objective functions and horizontal and vertical directions, it can

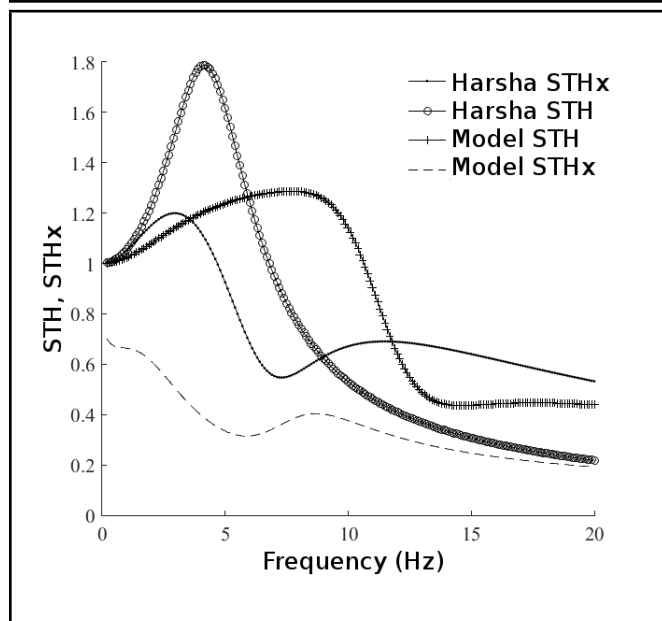


Figure 8. Compare optimization of horizontal and vertical vibrations transmission in the presented model by Harsha’s model with Eq. (8).

Table 10. The primary and optimal of seat stiffness and damping parameters for the presented model in Eq. (7).

| Parameter | Unit | Presented model | Optimal |
|-----------|------|-----------------|---------|
| k_{1v} | N/m | 1600 | 107013 |
| k_{1h} | N/m | 15 | 47 |
| k_{2v} | N/m | 151625 | 1057497 |
| k_{2h} | N/m | 905 | 7729 |
| k_{4v} | N/m | 17200 | 127102 |
| k_{4h} | N/m | 2300 | 240 |
| k_{5v} | N/m | 15000 | 2113 |
| k_{5h} | N/m | 4000 | 431 |
| c_{1v} | Ns/m | 104.35 | 436 |
| c_{1h} | Ns/m | 14 | 98 |
| c_{2v} | Ns/m | 47 | 208 |
| c_{2h} | Ns/m | 15 | 91 |
| c_{4v} | Ns/m | 334.5 | 1118 |
| c_{4h} | Ns/m | 154 | 17 |
| c_{5v} | Ns/m | 300 | 2605 |
| c_{5h} | Ns/m | 500 | 501 |

be concluded that the proposed model is desirable for minimizing head injuries caused by vibrations and to optimize the design of headrest parameters. However, the headrest has better performance in the horizontal direction in comparison with the vertical direction.

REFERENCES

- 1 Mansfield, N. J. *Human Response to Vibration*, CRC Press, Boca Raton, (2004). <https://dx.doi.org/10.1201/b12481>
- 2 Rasmussen, G. Human Body Vibration Exposure and Its Measurement, *Journal of the Acoustical Society of America*, **73** (6), 2229, (1983). <https://dx.doi.org/10.1121/1.389513>
- 3 Melikov, A., Ivanova, T. and Stefanova, G. Seat headrest-incorporated personalized ventilation: Thermal comfort and inhaled air quality, *Building and Environment*, **47** (1), 100–108, (2012). <https://dx.doi.org/10.1016/j.buildenv.2011.07.013>

- 4 Zhang, Z., Jin, K., Li, F., Lu, C., Chai, G. and Ye, D. Effects of adjustment devices on the fore-and-aft mode of an automobile seat system: Headrest, height adjuster, recliner and track slide, *Proceedings of the Institution of Mechanical Engineers, Part D: Journal of Automobile Engineering*, **230** (8), 1140–1152, (2016). <https://dx.doi.org/10.1177/0954407015602823>
- 5 Franz, M., Durt, A., Zenk, R. and Desmet, P. M. A. Comfort effects of a new car headrest with neck support, *Applied Ergonomics*, **43** (2), 336–343, (2012). <https://dx.doi.org/10.1016/j.apergo.2011.06.009>
- 6 Hamilton, A. A study of spastic anaemia in the hands of stone cutters, *Industrial Accident Hygiene Services Bulletin*, **236**, 53–66, (1918).
- 7 Gu, Y. A New Dummy for Vibration Transmissibility Measurement in Improving Ride Comfort, *SAE International*, (1999). <https://dx.doi.org/10.4271/1999-01-0629>
- 8 Alem, N. M., Nusholtz, G. S. and Melvin, J. W. Head and neck response to axial impacts, *SAE Technical Paper*, (1984). <https://dx.doi.org/10.4271/841667>
- 9 Boileau, P. É., Wu, X. and Rakheja, S. Definition of a range of idealized values to characterize seated body biodynamic response under vertical vibration, *Journal of Sound and Vibration*, **215** (4), 841–862, (1998). <https://dx.doi.org/10.1006/jsvi.1998.1674>
- 10 Yoganandan, N., Pintar, F. A., Stemper, B. D., Schlick, M. B., Philippens, M. and Wisnans, J. Biomechanics of human occupants in simulated rear crashes: documentation of neck injuries and comparison of injury criteria, *Stapp Car Crash Journal*, **44**, 189–204, (2000).
- 11 Mansfield, N. J. Impedance methods (apparent mass, driving point mechanical impedance and absorbed power) for assessment of the biomechanical response of the seated person to whole-body vibration, *Industrial Health*, **43** (3), 378–389, (2005). <https://dx.doi.org/10.2486/indhealth.43.378>
- 12 Néllisse, H., Patra, S., Rakheja, S., Boutin, J., and Boileau, P. E. Assessments of two dynamic manikins for laboratory testing of seats under whole-body vibration, *International Journal of Industrial Ergonomics*, **38** (5–6), 457–470, (2008). <https://dx.doi.org/10.1016/j.ergon.2007.10.029>
- 13 Bovenzi, M. A Longitudinal Study of Low Back Pain and Daily Vibration Exposure in Professional Drivers, *Industrial Health*, **48** (5), 584–595, (2010). <https://dx.doi.org/10.2486/indhealth.MSWBVI-02>
- 14 Thamsuwan, O., Blood, R. P., Ching, R. P., Boyle, L. and Johnson, P. W. Whole body vibration exposures in bus drivers: A comparison between a high-floor coach and a low-floor city bus, *International Journal of Industrial Ergonomics*, **43** (1), 9–17, (2013). <https://dx.doi.org/10.1016/j.ergon.2012.10.003>

Table 11. The comparison of the headrest adding effect.

| Objective function | Vibration direction | Harsha model (WO headrest) | Proposed model (W headrest) | Improvement (%) |
|---|-------------------------------|----------------------------|-----------------------------|-----------------|
| $y = 0.5 \cdot \text{RMS}(STH_x) + 0.5 \cdot \text{RMS}(STH)$ | Mixed vertical and horizontal | 0.51 | 0.49 | 3.9 |
| $y = 0.3 \cdot \text{RMS}(STH_x) + 0.7 \cdot \text{RMS}(STH)$ | Mixed vertical and horizontal | 0.61 | 0.55 | 9.8 |
| $y = \max(STH)$ | Vertical | 1.00 | 0.50 | 50 |
| $y = \text{RMS}(STH_x)$ | Horizontal | 0.48 | 0.24 | 50 |

- ¹⁵ Zhao, Y., Zhao, L. and Gao H. Vibration Control of Seat Suspension using H_∞ Reliable Control, *Journal of Vibration and Control*, **16** (12), 1859–1879, (2010). <https://dx.doi.org/10.1177/1077546309349852>
- ¹⁶ Zhou Z. and Griffin M. J. Response of the seated human body to whole-body vertical vibration: biodynamic responses to mechanical shocks, *Ergonomics*, **60** (3), 333–346, (2017). <https://dx.doi.org/10.1080/00140139.2016.1164902>
- ¹⁷ Jamali Shakhilavi S., Marzbanrad, J. and Tavooosi, V. Various vehicle speeds and road profiles effects on transmitted accelerations analysis to human body segments using vehicle and biomechanical models, *Cogent Engineering*, **5** (1), 1–17, (2018). <https://dx.doi.org/10.1080/23311916.2018.1461529>
- ¹⁸ Kociolek A. M., Lang, A. E., Trask, C. M., Vasiljev, R. M. and Milosavljevic, S. Exploring head and neck vibration exposure from quad bike use in agriculture, *International Journal of Industrial Ergonomics*, **66**, 63–69, (2018). <https://dx.doi.org/10.1016/j.ergon.2018.02.009>
- ¹⁹ Wu, J. Z., Welcome, D. E., McDowell, T. W., Xu, X. S. and Dong, R. G. Modeling of the interaction between grip force and vibration transmissibility of a finger, *Medical Engineering & Physics*, **45**, 61–70, (2017). <https://dx.doi.org/10.1016/j.medengphy.2017.04.008>
- ²⁰ Ambrosio, J. Interactions between mechanical systems and continuum mechanical models in the framework of biomechanics and vehicle dynamics, in *Advances in Mechanics: Theoretical, Computational and Interdisciplinary Issues - 3rd Polish Congress of Mechanics, PCM 2015 and 21st International Conference on Computer Methods in Mechanics, CMM 2015*, 3–10, (2016).
- ²¹ Fan, W. and Guo, L.-X. Finite element investigation of the effect of nucleus removal on vibration characteristics of the lumbar spine under a compressive follower preload, *Journal of the Mechanical Behavior of Biomedical Materials*, **78**, 342–351, (2018). <https://dx.doi.org/10.1016/j.jmbbm.2017.11.040>
- ²² Zhu, Q., Liu, L., Du, Y. and Chen, K. Human-induced vibration and control for cantilever steel bar truss deck slab based on pedestrain-structure interaction, *Jianzhu Jieqou Xuebao/Journal of Building Structures*, **39** (1), 99–108, (2018).
- ²³ Siefert, A. Occupant Vibrations - A Challenge for Seat Development, *SAE Technical Paper*, (2016). <https://dx.doi.org/10.4271/2016-01-1432>
- ²⁴ Zhang, Z., Ye, D., Li, F., Lu, C., Shao, M. and Jin, K. Experimental study of the influence levels of different vehicle seat adjustments on the fore-and-aft modal characteristics using the orthogonal array method, *Proceedings of the Institution of Mechanical Engineers, Part D: Journal of Automobile Engineering*, **232** (2), 212–219, (2018). <https://dx.doi.org/10.1177/0954407017694598>
- ²⁵ Harsha, S. P., Desta, M., Prashanth, A. S. and Saran, V. H. Measurement and bio-dynamic model development of seated human subjects exposed to low frequency vibration environment, *International Journal of Vehicle Noise and Vibration*, **10** (1–2), 1–24, (2014). <https://dx.doi.org/10.1504/IJNVN.2014.059627>
- ²⁶ Abbas, W., Abouelatta, O. B., El-Azab, M., El-saidy, M. and Megahed, A. A. Optimization of Biodynamic Seated Human Models Using Genetic Algorithms, *Engineering*, **2** (9), 710–719, (2010). <https://dx.doi.org/10.4236/eng.2010.29092>
- ²⁷ Gan, Z., Hillis, A. J. and Darling, J. Biodynamic modelling of seated human subjects exposed to uncouples vertical and fore-and-aft whole-body vibration, *Journal of Vibration Engineering and Technologies*, **3** (3), 301–314, (2015).
- ²⁸ Kim, S. K., White, S. W., Bajaj, A. K. and Davies, P. Simplified models of the vibration of mannequins in car seats, *Journal of Sound and Vibration*, **264** (1), 49–90, (2003). [https://dx.doi.org/10.1016/S0022-460X\(02\)01164-1](https://dx.doi.org/10.1016/S0022-460X(02)01164-1)
- ²⁹ Goldberg, D. *Genetic algorithms in search, optimization, and machine learning*, Addison-Wesley Longman Publishing, Boston, (1989).
- ³⁰ Holland, J. Genetic algorithms, *Scientific American*, **267** (1), 66–73, (1992).
- ³¹ Masih-Tehrani, M. and Ebrahimi-Nejad, S. Hybrid Genetic Algorithm and Linear Programming for Bulldozer Emissions and Fuel-Consumption Management Using Continuously Variable Transmission, *Journal of Construction Engineering and Management*, **144** (7), (2018). [https://dx.doi.org/10.1061/\(ASCE\)CO.1943-7862.0001490](https://dx.doi.org/10.1061/(ASCE)CO.1943-7862.0001490)
- ³² Masih-Tehrani, M. and Dahmardeh, M. A Novel Power Distribution System Employing State of Available Power Estimation for a Hybrid Energy Storage System, *IEEE Transactions on Industrial Electronics*, **65** (8), 6676–6685, (2018). <https://dx.doi.org/10.1109/tie.2017.2774721>
- ³³ Griffin, M. J., *Handbook of human vibration*, Academic press, 2012.